His^{166} Is Critical for Active-Site Proton Transfer and Phototaxis Signaling by Sensory Rhodopsin I

Xue-Nong Zhang and John L. Spudich
Department of Microbiology and Molecular Genetics, University of Texas Medical School, Houston, Texas 77030 USA

ABSTRACT Photoinduced deprotonation of the retinylidene Schiff base in the sensory rhodopsin I transducer (SRI-HtrI) complex results in formation of the phototaxis signaling state S_{373}. Here we report identification of a residue, His^{166}, critical to this process, as well as to reprotonation of the Schiff base during the recovery phase of the SRI photocycle. Each of the residue substitutions A, D, G, L, S, V, or Y at position 166 reduces the flash yield of S_{373}, to values ranging from 2% of wild type for H166Y to 23% for H166V. The yield of S_{373} is restored to wild-type levels in HtrI-free H166L by alkaline deprotonation of Asp^{76}, a Schiff base proton acceptor normally not ionized in the SRI-HtrI complex, showing that proton transfer from the Schiff base in H166L occurs when an acceptor is made available. The flash yield and rate of decay of S_{373} of the mutants are pH dependent, even when complexed with HtrI, which confers pH insensitivity to wild-type SRI, suggesting that partial disruption of the complex has occurred. The rates of S_{373} reprotonation at neutral pH are also prolonged in all H166X mutants, with half-times from 5 s to 160 s (wild type, 1 s). All mutations of His^{166} tested disrupt phototaxis signaling. No response (H166D, H166L), dramatically reduced responses (H166V), or inverted responses to orange light (H166A, H166G, H166S, and H166Y) or to both orange and near-UV light (H166Y) are observed. Our conclusions are that His^{166} 1) plays a role in the pathways of proton transfer both to and from the Schiff base in the SRI-HtrI complex, either as a structurally important residue or possibly as a participant in proton transfers; 2) is involved in the modulation of SRI photoreaction kinetics by HtrI; and 3) is important in phototaxis signaling. Consistent with the involvement of the His imidazole moiety, the addition of 10 mM imidazole to membrane suspensions containing H166A receptors accelerates S_{373} decay 10-fold at neutral pH, and a negligible effect is seen on wild-type SRI.

INTRODUCTION

Sensory rhodopsin I (SRI) is a 7-transmembrane helix retinylidene protein that mediates the phototactic behavior of *Halobacterium salinarum* (previously *halobium* and *salinarium*), a halophilic archeaon (Hoff et al., 1997). It is structurally and photochemically similar to the light-driven proton pump bacteriorhodopsin (BR) found in the same organism. In both proteins, the retinal chromophore is covalently bound via a protonated Schiff base linkage to the ϵ-amino group of a lysine residue in the midmembrane region of helix G. Photon absorption causes isomerization of the retinal and initiates a cyclic reaction during which the Schiff base undergoes deprotonation and reprotonation. Schiff base proton transfers are critical for proton transport by BR (Mathies et al., 1991; Oesterhelt et al., 1992; Rothschild, 1992; Ebrey, 1993; Krebs and Khorana, 1993; Lanyi, 1993) and have been implicated in the formation of SRI signaling states (Yan and Spudich, 1991; Spudich, 1994).

In BR (λ_{max} 568 nm) vectorial proton translocation depends on the interaction of ionizable residues with the Schiff base. In the dark a cluster consisting of three residues, Arg^{82}, Asp^{85}, and Asp^{212}, provides a net single negative charge counterion to the Schiff base proton (De Groot et al., 1989; Der et al., 1991; Marti et al., 1992). Asp^{85}, which is part of a proton release path to the extracellular medium, accepts the Schiff base proton in the first part of the pumping cycle (Braiman et al., 1988; Fahmy et al., 1992; Subramaniam et al., 1992). Asp^{96}, a residue located in the cytoplasmic portion of the protein, reprotonates the Schiff base nitrogen after a conformational change that switches the Schiff base accessibility to the cytoplasmic side (Otto et al., 1989; Tittor et al., 1989).

In SRI (λ_{max} 587 nm), Schiff base deprotonation accompanies formation of the SRI attractant signaling state, S_{373} (the subscript designates the absorption maximum) (Yan and Spudich, 1991; Haupts et al., 1994). The attractant response of the cell to orange light is proportional to the concentration of S_{373} produced by the photostimulus (Marwan et al., 1995). S_{373} thermally returns to the prestimulus SR_{587} in seconds. Photoexcitation of S_{373} drives it more rapidly to the reprotonated SR_{587} state in a process that induces swimming reversals (the repellent response) (Spudich and Bogomolni, 1984). It has therefore been suggested that residues participating in deprotonation and reprotonation of the Schiff base play a role in signaling by SRI (Spudich, 1994).

In the search for such residues, Arg^{73}, Asp^{76}, and Asp^{201}, which correspond in the SRI sequence (Blanck et al., 1989) to the residues of the protonated Schiff base counterion in BR, have been studied by site-directed mutagenesis. None was found to be critical for Schiff base proton transfers in SRI, nor were they critical for phototaxis (Olson et al.,

Received for publication 19 February 1997 and in final form 9 June 1997.

Address reprint requests to Dr. John L. Spudich, Department Microbiology/ Molecular Genetics, University of Texas Medical School, Health Science Center, JFB1.710, 6431 Fannin St., Houston, TX 77030. Tel.: 713-500-5458, ext. 1522; Fax: 713-500-5499; E-mail: spudich@utmmg.med.uth.tmc.edu.

0006-3495/97/09/1516/08 $2.00

1995). In particular, Asp^{76}, in the homologous position as the Schiff base proton acceptor Asp^{85} in BR and as the acceptor Asp^{73} in sensory rhodopsin II (SRII, Spudich et al., 1997), is not ionized and hence is not a proton acceptor in sensory signaling SRI (Rath et al., 1994). (However, Asp^{76} is the primary proton acceptor from the Schiff base in the blue-shifted proton pumping form of HtrI-free SRI (Rath et al., 1996).) Asp^{76} is also not necessary for phototaxis, because both D76A and D76N exhibited responses to orange light and to near-UV light in an orange light background (Rath et al., 1994). Although D201N produces an inverted response to orange light, showing it is positioned at a sensitive site (Olson et al., 1995), D201A and D201E nevertheless behave like wild type (unpublished observations).

Deprotonation of the Schiff base in SRI, therefore, may be determined by residues that are not conserved in BR or SRII. His^{166} (Fig. 1) in SRI stands out because it is a protonatable residue in or near the retinal binding pocket that is not conserved in BR or SRII (corresponding residues are a valine in BR (Henderson et al., 1990) and an isoleucine in SRII (Zhang et al., 1996)). Here we report an analysis of a series of residue replacements at position 166 which demonstrates that His^{166} is crucial for both proton transfers and phototaxis signaling.

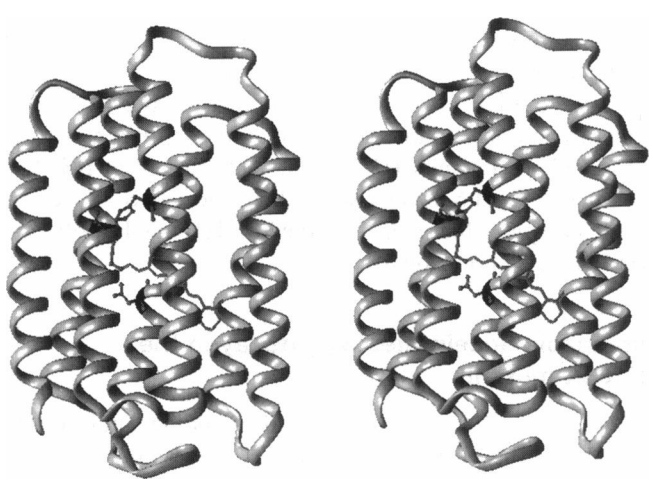

FIGURE 1 Stereo view illustrating the approximate positions of His^{166} and Asp^{76} in sensory rhodopsin I (SRI), as predicted from homology with bacteriorhodopsin (BR). The ribbon backbone is that of the seven helices of the BR protein (coordinates from Grigorieff et al., 1996), in which the homologous residue Val^{177} only has been substituted by a histidine residue with the program Insight II (Biosym/Molecular Simulations, San Diego, CA). The protonated nitrogen of the Schiff base is the final atom (*ball-and-stick appearance*) attached to the retinal (*stick appearance*) near the middle of the structure. The upper surface is cytoplasmic and the bottom periplasmic. The precise positions of His^{166} (above retinal on helix F; front helix in stereo view) and Asp^{76} (below retinal; back helix in stereo view) are not known for SRI, and the prediction from the BR structure shown here should be considered only a first approximation.

MATERIALS AND METHODS

Strains and plasmids

Native and mutant forms of SRI were expressed by transformation of *H. salinarum* strains Flx15Δ*sopI* ($SRI^{-}HtrI^{+}$) (Krebs et al., 1993) and Pho81Wr^{-} ($SRI^{-}HtrI^{-}$) (Yao et al., 1994), using polyethylene glycol-mediated spheroplast transformation (Cline and Doolittle, 1987). Polymerase chain reaction (PCR)-based site-specific mutagenesis was carried out according to the method of Chen and Przybyla (1994). A 933-bp *PstI*/*Eco*RV fragment from the native *htrI* gene and 630-bp *Bam*HI/*Not*I fragment from the synthetic *sopI* gene (Krebs et al., 1993) were first cloned into pBluescript KS^{-} (Stratagene, La Jolla, CA) and used as the template for the PCR. T3, T7 primers and synthetic oligonucleotides (Bioserve, Laurel, MD) containing the desired mutations were used as PCR primers. Reactions were performed in a programmable thermal controller 100 (MJ Research, Watertown, MA) at 94°C, 1 min; 50°C, 1 min; and 72°C, 1 min for 31 cycles. PCR fragments were purified from agarose gel with a glass powder-based method (Boom et al., 1990). After digestion by appropriate enzymes, the fragment was replaced in pVJY1 (Yao et al., 1994) or pTR2 (Olson and Spudich, 1993). The mutations were confirmed by sequencing. *Escherichia coli* strain DH5α (Stratagene, Menasha, WI) was used for plasmid manipulation and amplification.

Cell tracking and motion analysis

Motility responses to SRI photoactivation were assayed by computer-assisted cell tracking and motion analysis as described (Krebs et al., 1993). For fluence response study, the light intensity at different wavelengths selected by 10-nm bandwidth interference filters and neutral density filters (Corion, Holliston, MA) was measured at the position of the sample chamber with a radiometer (Kettering model 68; Scientific Instruments, West Palm Beach, FL). Fine adjustment of the light output from the tungsten/halogen lamp was made with a variable-output transformer (Fisher Scientific, Pittsburgh, PA). Pulse durations were controlled by a Uniblitz electronic shutter (Vincent Associates, Rochester, NY). Phototaxis stimuli were delivered through an epiilluminator from a Nikon 100-W Hg/Xe or from a 150-W tungsten/halogen lamp beam conducted to the epiilluminator via fiber optics.

Membrane preparations

The membrane fraction was isolated from sonicated early stationary phase cells as described (Olson et al., 1995). Membrane suspensions were in 4 M NaCl/25 mM Tris-HCl (pH 6.8). Wet membrane pellets prepared by centrifuging for 20 min at 75,000 rpm in a Beckman TL-100 tabletop ultracentrifuge were mounted in a 0.2-mm or 0.5-mm dismountable cuvette (Starna Cells, Atascadero, CA). To prevent dehydration, cuvettes were sealed with parafilm. Freshly made pellets were used for each study.

Spectroscopy

Flash-induced absorbance changes of pigments were measured with a laboratory-constructed cross-beam kinetic spectrophotometer (Spudich et al., 1986) in membrane suspensions (1-cm pathlength) or with an RSM-1000 spectrometer (On-Line Instrument Systems, Bogart, GA), using membrane pellets (0.2-mm or 0.5-mm pathlength). The actinic flash was from a Nd-YAG pulse laser (532 nm, 6-ns duration, 40 mJ; Surelite I, Continuum, Santa Clara, CA). For the measurement of the light-induced absorption difference spectrum of the highly photolabile H166R, membrane pellets containing the mutant receptor and HtrI were dark-adapted overnight and placed in the sample chamber of the RSM-1000 spectrometer. After a baseline was recorded, the difference spectrum induced by the monitoring light was recorded. Membranes containing wild-type and mutant receptors were bleached by mixing with an equal volume of 1 M NH_2OH (pH 9.0) and illuminated with orange light for 1 h. Bleached

membranes were washed extensively and reconstituted by adding 1-μl increments of 60 μM ethanolic solution of retinal to 2 ml membrane suspension until no further increase in the pigment peak was observed. Absorption spectra were recorded on a DW-2000 UV-Vis spectrophotometer (SLM Instruments, Urbana, IL). All measurement were carried out at 18 ± 0.5°C. Flash photolysis data were fit by a single-exponential function with the curve-fitting program from SIGMAPLOT (Jandel, San Rafael, CA).

RESULTS

Mutations of His^{166} inhibit production of S_{373} and prolong S_{373} decay

The yields of S_{373} of SRI H166X mutants and native SRI expressed in the presence of HtrI were monitored at pH 6.8 at 400 nm after a 532-nm laser flash (Table 1). The effect of single amino acid substitutions of His^{166} was to reduce the flash yield of S_{373} to values ranging from 2% to 23%. Because of the low yields of S_{373} and relatively low signal-to-noise in the submillisecond to millisecond range, S_{373} formation rates in the mutants were difficult to quantitate, but their main components did not appear to be greatly reduced from the ~300-μs rate of wild type. Absorption spectra of these mutant SRI were obtained by bleaching with NH_2OH and reconstituting with all-*trans*-retinal. All exhibit maxima near 590 nm, like wild-type SRI, except for H166D and H166Y, which are slightly red-shifted, and H166R, which is significantly blue-shifted (Table 1). The expression levels of the mutant receptors were all about the same and were similar to that of wild-type SRI, as evidenced by absorption measurements (data not shown).

To assess the decay rate of S_{373}, 2-s continuous orange light (600 nm) was used as actinic light to accumulate S_{373}. Wild-type SRI exhibited a $t_{1/2}$ of S_{373} decay of 1 s after the illumination period. H166X mutations all prolonged this process with S_{373} decay half-times varying from 5 s to 160 s (Fig. 2). It has been observed that in the absence of the HtrI transducer, the lifetime of S_{373} is prolonged at neutral pH (Spudich and Spudich, 1993). Mutants H166R, H166Y, H166L, and H166A, in the presence of HtrI, all have an even longer $t_{1/2}$ than that of the wild-type SRI in the absence of HtrI (Fig. 2). Furthermore, in H166L, removal of HtrI did not further prolong the $t_{1/2}$ of S_{373} decay (Fig. 2). Hence the modulating effect by HtrI over S_{373} decay was eliminated in this mutant.

TABLE 1 Relative flash yield of S_{373} and absorption maxima of H166X mutants

Substitution	Relative flash yield (%)	Absorption maximum (nm)
Wild type	100	587
H166A	10	590
H166D	9	596
H166G	9	590
H166L	7	588
H166R	*	552
H166S	9	586
H166V	23	588
H166Y	2	602

*Not measured because of pigment photolability.

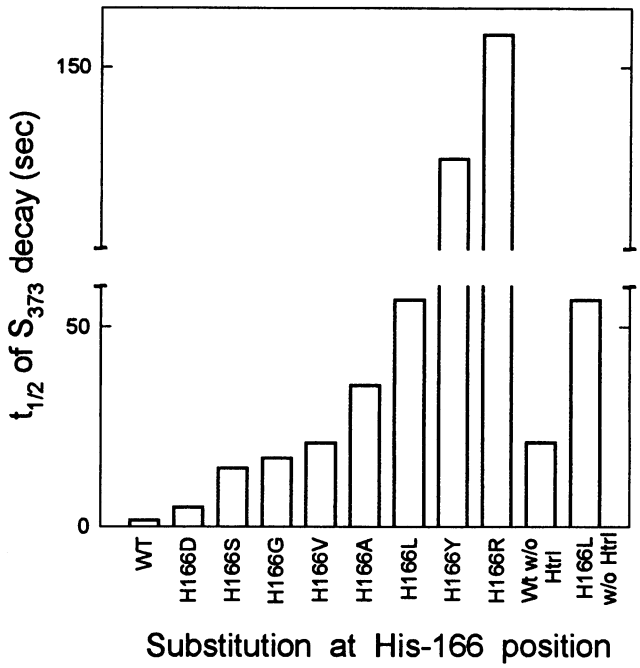

FIGURE 2 Half-life of S_{373} decay of the wild-type and H166X mutants in the presence and in the absence of the transducer HtrI. Membrane pellets suspended in 4 M NaCl, 25 mM Tris-HCl (pH 6.8) were subjected to 2-s illumination at 600 ± 20 nm. Absorption transients, monitored at 400 nm after the actinic light was turned off, were fit to a single-exponential decay.

Both the decay rate and yield of S_{373} in H166X mutants in the presence of HtrI were pH sensitive. At pH 9 all H166X mutants except H166R had three- to fivefold higher S_{373} yield than at pH 6.8. Furthermore, more complex kinetics and one- to threefold increased S_{373} lifetimes were observed for mutants H166A, G, L, S, and V at pH 9 as compared to pH 6.8. Only slight differences in S_{373} lifetime at the two pH values were observed for H166D, H166R, and H166Y (data not shown).

Imidazole accelerates S_{373} decay in the H166A mutant

The decay of S_{373} was assessed after adding imidazole to membrane suspensions containing H166A. Imidazole accelerated both S_{373} formation and decay in H166A membranes. Whereas no effect was seen on wild-type SRI at 10 mM, S_{373} decay in H166A membranes became 10-fold faster (Fig. 3).

The H166L mutant exhibits a wild-type S_{373} flash yield when Asp^{76} is provided as a proton acceptor

The reduced S_{373} flash yields of H166X mutants could be caused by 1) an increased pK_a of the Schiff base due to structural changes caused by the mutations or, alternatively,

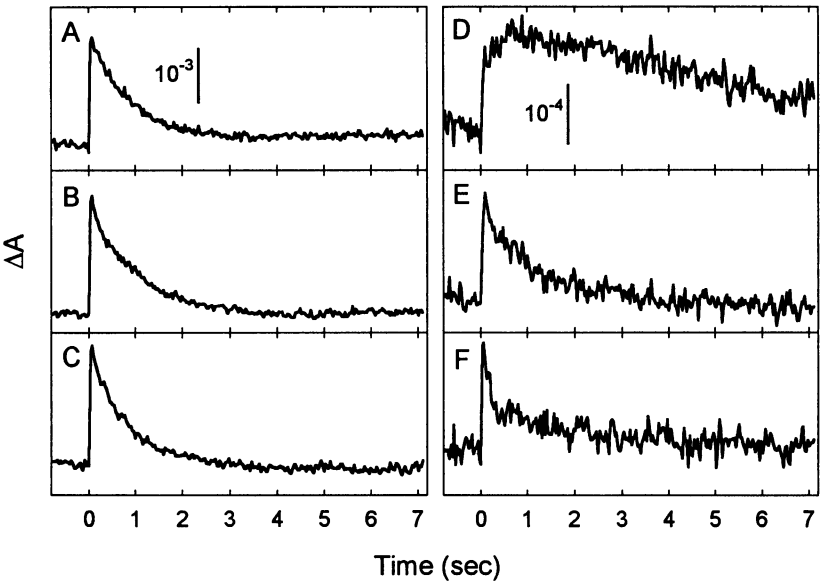

FIGURE 3 Laser flash-induced absorption transients at 400 nm in membrane suspensions from wild type (*A–C*) and the H166A mutant (*D–F*) in the presence of HtrI. Membrane suspensions in 4 M NaCl, 25 mM Tris-HCl (pH 6.8), with no imidazole (*A*, *D*), with 10 mM imidazole (*B*, *E*), and with 100 mM imidazole (*C*, *F*) were subjected to a 6-ns flash at 532 nm at time 0. The length of the bar indicates 10^{-3} and 10^{-4} absorbance units in *A–C* and *D–F*, respectively.

by 2) disruption of the deprotonation pathway. To distinguish these possibilities we compared H166L and wild-type SRI under conditions in which the deprotonation pathway is replaced by Asp^{76}, the proton acceptor in the 552-nm (purple) form of SRI (Rath et al., 1996). In HtrI-free membranes, wild-type SRI and H166L exhibited blue-to-purple transitions with an identical pK_a of 7.6 (Fig. 4 *B*). In wild-type SRI this transition is known to be caused by deprotonation of Asp^{76}, which introduces a strong counterion near the Schiff base that shifts the absorption to shorter wavelengths (Rath et al., 1996). Whereas the S373 yield of H166L is <10% of that of wild-type SRI at pH ≤ 5, the relative yield increases to ~100% at higher pH (Fig. 4 *A*, *inset*), as the purple (552 nm) form is generated (Fig. 4 *B*). Our interpretation is that the Schiff base of H166L deprotonates normally when the alternative acceptor Asp^{76} is provided, and that the reduced yield at lower pH suggests the need for His^{166} in the deprotonation path in the native blue (587 nm) pigment, in which Asp^{76} is not ionized.

Phototaxis signaling

SRI mediates attractant responses to orange light by photoexcitation of SR_{587} and repellent responses to near-UV light in an orange light background by photoexcitation of S_{373}. The residue substitutions of His^{166} dramatically affect these phototaxis responses, causing a variety of aberrant phenotypes (Fig. 5).

Inverted signaling to orange light, as has been reported for D201N, was observed for H166A, H166G, H166S, and H166Y. Orange light is normally an attractant, i.e., the

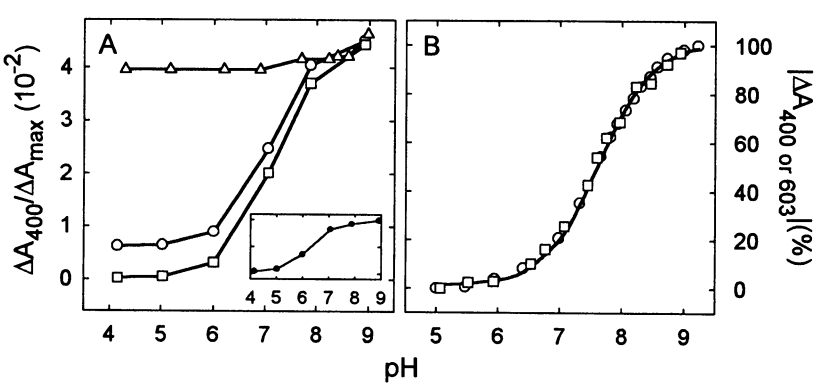

FIGURE 4 Correspondence of relative S_{373} yield and pH titration of Asp^{76} in H166L. (*A*) pH dependence of S_{373} yield in wild-type SRI (○), H166L (□) in the absence of the transducer, and wild-type SRI in the presence of the transducer (△). Maximum absorption changes at 400 nm after a 6-ns laser flash at 532 nm, expressed per total amount of pigment present in the sample, were plotted against pH. (*Inset*) Fractional S_{373} yield of H166L in the absence of HtrI relative to that of the wild type in the absence of HtrI. The ordinate tick marks are at 0, 0.5, and 1.0. Values range from 0.04 at pH 4 to 0.99 at pH 9. (*B*) pH titration of the blue (λ_{max} 587 nm) to purple (λ_{max} 552 nm) transition (○) and S_{373} yield (□) by membrane containing H166L in the absence of HtrI. pH-induced absorbance changes were measured at 603 nm. S_{373} formation after the flash was monitored at 400 nm. The solid line is the fit to a monoprotic titration with pK_a 7.6. pH titrations were carried out by adding diluted HCl or NaOH in microliter amounts.

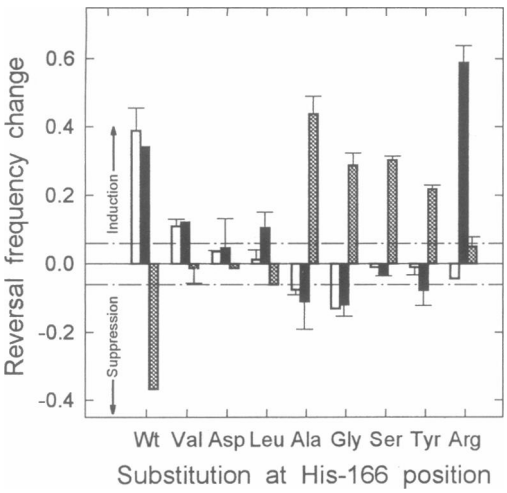

FIGURE 5 Phototaxis responses of wild type and H166X mutants. Three stimuli were delivered: a 600-nm step-down stimulus consisting of 4-s removal of 600 ± 20 nm light (□), a 400-nm stimulus consisting of a 20-ms, 400-nm pulse under continuous orange light background illumination (■), and a 600-nm step-up stimulus consisting of 4 s of 600 ± 20 nm light (▨). The phototaxis index is calculated in s^{-1}, as the integral of the reversal frequency measured by motion analysis for the first 2 s after the stimuli minus the integral of 2 s starting from 6 s after the stimuli were initiated. Attractant stimuli produce negative index values (suppression), and repellent stimuli produce positive index values (induction). Reference lines (*dash-dotted lines*) indicate the noise envelope in the measurement.

wild-type response to orange light is suppression of reversals. For these four mutants, a step up in orange light induced swimming reversals. Unlike D201N, which still exhibits normal repellent responses to near-UV light, H166A, H166G, H166S, and H166Y lost this response.

When His^{166} was substituted with Arg, the orange light response was eliminated, and cells carrying this mutation were hypersensitive to near-UV light. H166R had the longest S_{373} lifetime, with a $t_{1/2}$ of S_{373} decay of ~160 s (Table 1), and therefore S_{373} accumulates in high concentrations under continuous orange light illumination. The observed hypersensitivity to repellent near-UV light is likely to be due to this effect, because S_{373} is the repellent receptor form of SRI.

H166V was the only substitution that retained (weakened) wild-type responses. Reversal responses to a step down in attractant light and step up in repellent light by cells containing H166V were each reduced to ~30% of that of wild type, with a 1–1.5-s delay in the response after stimulation. H166V was also the substitution permitting the highest yield of S_{373} among the mutants (Table 1). Substitution of His^{166} with Asp or Leu, which reduce S_{373} yield to <10%, nearly abolished phototaxis responses to both attractant and repellent stimuli (Fig. 5).

Doubly inverted signaling mutants

In the case of H166Y, a step down of near-UV light (400 nm) induced reversals in an orange light-dependent manner, indicating that the step down in S_{373} photoexcitation mediates this response (Fig. 6 *D*). The response is opposite to that of the wild type (Fig. 6 *C*). Reversals induced by near-UV light step-down stimuli were also observed for H166A, H166G, and H166S, although much smaller signals were obtained (data not shown). Inverted responses (reversal suppression) of H166A, G, S, and Y were also observed after near-UV pulse stimuli (Fig. 5). Kinetic analysis of flash-induced absorption transients showed in the case of H166Y a maximum absorption change at ~500 nm, indicating an L-like intermediate rising with a $t_{1/2}$ of 100 μs, similar to that of the wild type, and then decaying with a $t_{1/2}$ of ~10 ms, the same as the main component in the regeneration rate of the unphotolyzed form (Fig. 6 *B*). The flash-induced absorption difference spectrum of H166Y also indicates formation of an L-like intermediate (Fig. 7). All H166X mutants that gave an orange light inverted response were observed to accumulate similar L-like intermediates, whereas nonresponding and weak wild-type responding mutants accumulated L-like intermediates to a much lesser extent. Therefore accumulation of the L-like intermediate is correlated with the inverted response. Fluence response curves show that 400-nm light is more effective than 450-nm light in eliciting this response (data not shown), indicating that the photoreceptor for the inverted behavior in these mutants is not the accumulated L-like intermediate itself, but rather S_{373}.

DISCUSSION

Proton transfers involving the Schiff base are likely to be important in SRI signaling because 1) deprotonation occurs

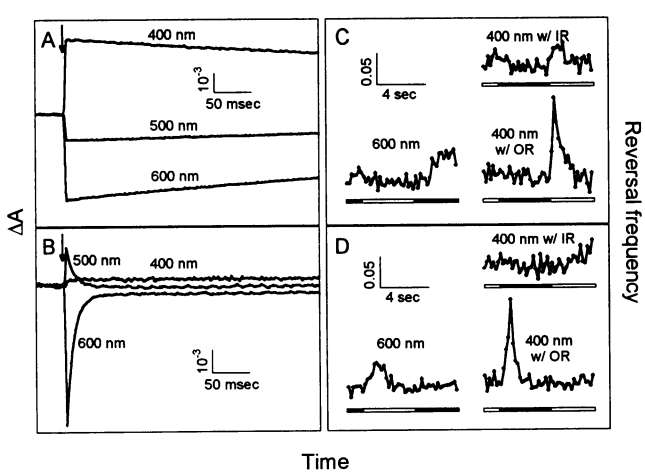

FIGURE 6 Comparison of flash-induced absorption transients (*A*, *B*) and phototaxis behavior (*C*, *D*) of wild-type SRI (*A*, *C*) and H166Y (*B*, *D*). Transients in wet membrane pellets at 400 nm, 500 nm, and 600 nm were monitored after a 6-ns flash at 532 nm at the arrow (*A*, *B*). Phototaxis responses to a 4-s, 600-nm pulse (*C, D left half*), and to a 4-s, 400-nm pulse (*C, D right half*) in the absence of orange light (*C, D right upper*) and in the presence of orange light (*C, D right lower*) are shown. Bars under the response transients indicate the time period during which the light was on (*white region*) or off (*black region*).

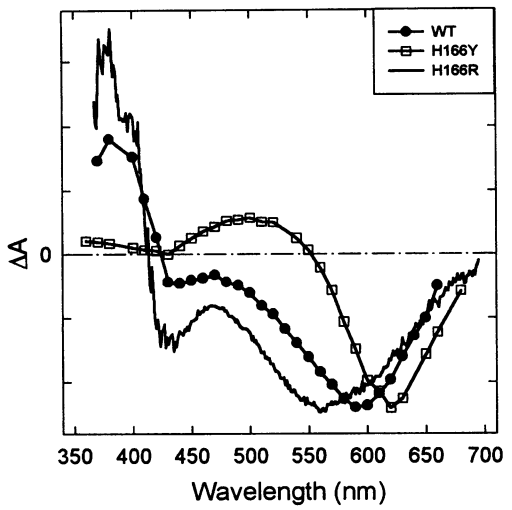

FIGURE 7 Light-induced absorption difference spectra. Membrane suspensions containing HtrI and wild-type SRI (●) or H166Y (□) in 4 M NaCl, 25 mM Tris-HCl (pH 6.8) were subjected to a 532-nm laser flash, and absorption transients were monitored at various wavelengths. Absorption changes at 1 ms after the flash were plotted. The light-induced difference spectrum of H166R (*solid line*) was obtained as described in Materials and Methods by using wet membrane pellets. Maximum absorption depletions were 1.1×10^{-2}, 7.8×10^{-3}, and 9.3×10^{-3} absorbance units for wild-type, H166Y, and H166R, respectively. Spectra were normalized at their maximum depletion for plotting.

during formation of the attractant signaling state S_{373} (Yan and Spudich, 1991; Haupts et al., 1994) and 2) light-induced reprotonation occurs during repellent signaling by photoactivation of S_{373} (Spudich and Bogomolni, 1984). Moreover, 3) HtrI binding facilitates photoinduced deprotonation and blocks proton release from the complex, suggesting that HtrI is coupled to SRI proton transfer pathways (Spudich and Spudich, 1993; Olson and Spudich, 1993). The results presented here strengthen this correlation, because His^{166} mutations greatly perturb both Schiff base proton transfers and phototaxis signaling.

His^{166} controls both protonation and deprotonation in the SRI photocycle

In BR, deprotonation and reprotonation of the Schiff base are controlled by different residues. Asp^{85} is the major counterion of the protonated Schiff base and accepts the Schiff base proton during formation of M, the photocycle intermediate corresponding to S_{373}. Mutants D85A and D85N dramatically slow and reduce M formation (Otto et al., 1990). Asp^{96} is the principal residue in the Schiff base reprotonation pathway, and mutations at this position retard M decay by two orders of magnitude (Holz et al., 1989; Otto et al., 1989). Residues that strongly affect both M formation and decay have not been described for BR. Therefore the influence of His^{166} on both S_{373} formation and decay in SRI presents a marked difference between BR and SRI and raises the possibility that the same proton translocation pathway is responsible for both deprotonation and reprotonation of the Schiff base in SRI.

Previous measurements have established that the photocycle of HtrI-complexed SRI is nonelectrogenic (Ehrlich et al., 1984; Olson et al., 1992), and therefore the proton translocation pathway is an electroneutral circuit. One possibility is that His^{166} serves as a proton relay component in both the deprotonation and reprotonation portions of the circuit. A proton relay function of histidine has been described in the charge relay system of serine proteases (Blow et al., 1969; Frey et al., 1994). A similar role of His^{166} in proton relay would predict histidine protonation changes, possibly detectable by Fourier transform infrared spectroscopy, during the SRI photocycle. We emphasize, however, that our study does not demonstrate direct participation of His^{166} in proton transfer reactions. Alternatively, the data are fully consistent with a structural role of His^{166} that is important to proton transfers between other residues. Supporting this alternative is the less perturbed behavior of the H166V mutant, despite the absence of a protonatable residue at position 166.

In the H166X mutants the S_{373} formation rates are not greatly perturbed and S_{373} decay is slower than in wild type, favoring S_{373} accumulation after the flash. The reduced S_{373} yields therefore must be explained by other changes in the photocycle. One possibility is a branching of the photocyle before S_{373} formation. Supporting this explanation, most of the substitutions result in the appearance of long-lived, blue-shifted (L-like) intermediates, as is evident for H166L in Figs. 6 *B* and 7, and many also produce long-lived, red-shifted (K-like) intermediates (data not shown). Other explanations for the reduced but nonzero yields are conformational heterogeneity in the SRI ground state shifted by the mutations toward the population that does not produce S_{373}, and an alternative weakly active proton acceptor in the mutants (e.g., Asp^{76}).

His^{166} is the first residue mutated in SRI that eliminates or greatly perturbs all of its signaling modes

Mutation of residues in SRI chosen for their likely proximity to the Schiff base (Arg^{73}; Asp^{76}, Tyr^{87}; Asp^{106}, Asp^{201}; Olson et al., 1995) had relatively minor effects on de/reprotonation, and only one mutant, D201N, affected signaling. This substitution inverted the attractant signal, but left the repellent signal intact. However, Asp^{201} is not essential for the attractant signal, because D201A and D201E both mediate wild-type responses (unpublished observations). In contrast, nearly all substitutions of His^{166} greatly perturb de- and reprotonation and either eliminate signaling or elicit inverted responses to both normally attractant and repellent photostimuli. Only H166V produces normal-mode phototaxis responses (although weak and delayed), and H166V is the only mutation permitting significant (23% of wild type) S_{373} yield. Thus His^{166} is the first

residue identified to be critical for phototaxis signaling in SRI, and despite the expectation that its location would be distant from the protonated Schiff base nitrogen, as discussed below, it is also found to be critical to deprotonation and reprotonation of the Schiff base.

His^{166} corresponds to Val^{177} in BR, which is located in the cytoplasmic half of the membrane in helix F facing away from the retinal binding pocket between helices F and G (Fig. 1; Henderson et al., 1990; Grigorieff et al., 1996). Electron, neutron, and x-ray diffraction analysis revealed that helix F undergoes prominent movements during the BR photocycle, with the cytoplasmic part tilting away from the channel during the formation of M and N (Dencher et al., 1989; Koch et al., 1991; Nakasako et al., 1991; Subramaniam et al. 1993; Steinhoff et al., 1994; Ludlam et al., 1995; Kamikubo et al., 1996; Vonck, 1996). Recently, the movement of helix F relative to helix C has been suggested to also be important to the activation of mammalian rhodopsin (Farrens et al., 1996; Sheikh et al., 1996). Given the structural similarity between SRI and BR and the capacity of HtrI-free SRI to carry out BR-like proton translocation (Bogomolni et al., 1994), a similar conformational change is expected to occur in SRI. Therefore, helix F might provide the major interaction face that transmits the conformational change from SRI to HtrI. Genetic data also support this idea: mutations in SRI that are located in F and G suppress the inverted signaling by the E56Q mutant of HtrI (Jung and Spudich, 1996; Jung and Spudich, unpublished observations).

It is plausible that His^{166} in SRI functionally connects the protonation state of the Schiff base (possibly by interacting with a PSB counterion) to that of a group on HtrI that triggers the conformational switch. The substitution of arginine, expected to place a positive charge at position 166, shifts the absorption maximum over 1000 cm^{-1} to the blue, as measured by bleaching and reconstitution (Table 1) and as indicated by the depletion maximum of the H166R light-induced difference spectrum (Fig. 7). This argues that His^{166} can interact with the protonated Schiff base environment.

The histidine imidazole ring may undergo protonation changes, as occur in a variety of systems (Fersht, 1977; Shimoni et al., 1993; Ren et al., 1995; Rao et al., 1996) during the SRI signaling process. Protonation changes in the histidine imidazole have been well characterized in the charge relay system in serine proteases (Blow et al., 1969; Frey et al., 1994). Consistent with such a role of His^{166}, the addition of imidazole to H166A accelerates the return of the proton to the Schiff base during S_{373} decay. Given its location in the suspected conformationally active region between helices F and G on the cytoplasmic side of the protein, His^{166} may alternatively play an important structural role in the positioning of other residues directly involved in proton transfer reactions.

We thank Wouter Hoff, Kwang-Hwan Jung, Bastianella Perazzona, and Elena Spudich for many stimulating discussions.

This work was supported by National Institutes of Health grant R01-GM27750 (to JLS).

REFERENCES

Blanck, A., D. Oesterhelt, E. Ferrando, E. S. Schegk, and F. Lottspeich. 1989. Primary structure of sensory rhodopsin I, a prokaryotic photoreceptor. *EMBO J.* 8:3963–3971.

Blow, D. M., J. J. Birktoft, and B. S. Hartley. 1969. Role of a buried acid group in the mechanism of action of chymotrypsin. *Nature.* 221: 337–340.

Bogomolni, R. A., W. Stoeckenius, I. Szundi, E. Perozo, K. D. Olson, and J. L. Spudich. 1994. Removal of transducer HtrI allows electrogenic proton translocation by sensory rhodopsin I. *Proc. Natl. Acad. Sci. USA.* 91:10188–10192.

Boom, R., C. J. A. Sol, M. M. M. Salimans, C. L. Jansen, P. M. E. Wertheim-van Dillen, and J. van der Noordaa. 1990. Rapid and simple method for purification of nucleic acids. *J. Clin. Microbiol.* 28:495–503.

Braiman, M. S., T. Mogi, T. Marti, L. J. Stern, H. G. Khorana, and K. J. Rothschild. 1988. Vibrational spectroscopy of bacteriorhodopsin mutants: light-driven proton transport involves protonation changes of aspartic acid residues 85, 96, and 212. *Biochemistry.* 27:8516–8520.

Chen, B., and A. E. Przybyla. 1994. An efficient site-directed mutagenesis method based on PCR. *BioTechniques.* 17:657–659.

Cline, S. W., and W. F. Doolittle. 1987. Efficient transformation of the archaebacterium *Halobacterium halobium*. *J. Bacteriol.* 169:1341–1344.

De Groot, H. J., G. S. Harbison, J. Herzfeld, and R. G. Griffin. 1989. Nuclear magnetic resonance study of the Schiff base in bacteriorhodopsin: counterion effects on the ^{15}N shift anisotropy. *Biochemistry.* 28:3346–3353.

Dencher, N. A., D. Dresselhaus, G. Zaccai, and G. Büldt. 1989. Structural changes in bacteriorhodopsin during proton translocation revealed by neutron diffraction. *Proc. Natl. Acad. Sci. USA.* 86:7876–7879.

Der, A., S. Szara, R. Toth-Boconadi, Z. Tokaji, L. Keszthelyi, and W. Stoeckenius. 1991. Alternative translocation of protons and halide ions by bacteriorhodopsin. *Proc. Natl. Acad. Sci. USA.* 88:4751–4755.

Ebrey, T. G. 1993. Light energy transduction in bacteriorhodopsin. *In* Thermodynamics of Membranes, Receptors and Channels. M. Jackson, editor. CRC Press, Boca Raton, FL. 353–387.

Ehrlich, B. E., C. R. Schen, and J. L. Spudich. 1984. Bacterial rhodopsins monitored with fluorescent dyes in vesicles and in vivo. *J. Membr. Biol.* 82:89–94.

Fahmy, K., O. Weidlich, M. Engelhard, J. Tittor, D. Oesterhelt, and F. Siebert. 1992. Identification of the proton acceptor of Schiff base deprotonation in bacteriorhodopsin: a Fourier-transform-infrared study of the mutant Asp85 → Glu in its natural lipid environment. *Photochem. Photobiol.* 56:1073–1083.

Farrens, D. L., C. Altenbach, K. Yang, W. L. Hubbell, and H. G. Khorana. 1996. Requirement of rigid-body motion of transmembrane helices for light activation of rhodopsin. *Science.* 274:768–770.

Fersht, A. 1977. Enzyme Structure and Mechanism. W. H. Freeman and Company, New York. 288–329.

Frey, P. A., S. A. Whitt, and J. B. Tobin. 1994. A low-barrier hydrogen bond in the catalytic triad of serine proteases. *Science.* 264:1927–1930.

Grigorieff, N., T. A. Ceska, K. H. Downing, J. M. Baldwin, and R. Henderson. 1996. Electron-crystallographic refinement of the structure of bacteriorhodopsin. *J. Mol. Biol.* 259:393–421.

Haupts, U., W. Eisfeld, M. Stockburger, and D. Oesterhelt. 1994. Sensory rhodopsin I photocycle intermediate SRI_{380} contains 13-*cis* retinal bound via an unprotonated Schiff base. *FEBS Lett.* 356:25–29.

Henderson, R., J. M. Baldwin, T. A. Ceska, F. Zemlin, E. Beckmann, and K. H. Downing. 1990. Model for the structure of bacteriorhodopsin based on high-resolution electron cryo-microscopy. *J. Mol. Biol.* 213: 899–929.

Hoff, W., K.-H. Jung, and J. L. Spudich. 1997. Molecular mechanism of photosignaling by archaeal sensory rhodopsins. *Annu. Rev. Biophys. Biomol. Struct.* 26:221–256.

Holz, M., L. A. Drachev, T. Mogi, H, Otto, A. D. Kaulen, M. P. Heyn, V. P. Skulachev, and H. G. Khorana. 1989. Replacement of aspartic acid-96 by asparagine in bacteriorhodopsin slows both the decay of the M intermediate and the associated proton movement. *Proc. Natl. Acad. Sci. USA.* 86:2167–2171.

Jung, K.-H., and J. L. Spudich. 1996. Protonatable residues at the cytoplasmic end of transmembrane helix-2 in the signal transducer HtrI control photochemistry and function of sensory rhodopsin I. *Proc. Natl. Acad. Sci. USA.* 93:6557–6561.

Kamikubo, H., M. Kataoka, G. Varo, T. Oka, F. Tokunaga, R. Needleman, and J. K. Lanyi. 1996. Structure of the N intermediate of bacteriorhodopsin revealed by x-ray diffraction. *Proc. Natl. Acad. Sci. USA.* 93: 1386–1390.

Koch, M. H. J., N. A. Dencher, D. Oesterhelt, H.-J. Plöhn, G. Rapp, and G. Büldt. 1991. Time-resolved X-ray diffraction study of structure changes associated with the photocycle of bacteriorhodopsin. *EMBO J.* 10: 521–526.

Krebs, M. P., and H. G. Khorana. 1993. Mechanism of light-dependent proton translocation by bacteriorhodopsin. *J. Bacteriol.* 175:1555–1560.

Krebs, M. P., E. N. Spudich, H. G. Khorana, and J. L. Spudich. 1993. Synthesis of a gene for sensory rhodopsin I and its functional expression in *Halobacterium halobium. Proc. Natl. Acad. Sci. USA.* 90:3486–3490.

Lanyi, J. K. 1993. Proton translocation mechanism and energetics in the light-driven pump bacteriorhodopsin. *Biochim. Biophys. Acta.* 1183: 241–261.

Ludlam, C., F. Sonar, S. Lee, C. P., Coleman, M., Herzfeld, J., Raj-Bhandary, U. L., and Rothschild, K. J. 1995. Site-directed isotope labeling and ATR-FTIR difference spectroscopy of bacteriorhodopsin: the peptide carbonyl group of Tyr 185 is structurally active during the bR→N transition. *Biochemistry.* 34:2–6.

Marti, T., H. Otto, S. J. Rosselet, M. P. Heyn, and H. G. Khorana. 1992. Anion binding to the Schiff base of the bacteriorhodopsin mutants Asp-85→Asn/Asp-212→Asn and Arg-82→Gln/Asp-85→Asn/Asp-212→Asn. *J. Biol. Chem.* 267:16922–16927.

Marwan, W., S. I. Bibikov, M. Montrone, and D. Oesterhelt. 1995. Mechanism of photosensory adaptation in *Halobacterium salinarium. J. Mol. Biol.* 246:493–499.

Mathies, R. A., S. W. Lin, J. B. Ames, and W. T. Pollard. 1991. From femtoseconds to of biology: mechanism of bacteriorhodopsin's light-driven proton pump. *Annu. Rev. Biophys. Biophys. Chem.* 20:491–518.

Nakasako, M., M. Kataoka, Y. Amemiya, and F. Tokunaga. 1991. Crystallographic characterization of X-ray diffraction of the M-intermediate from the photo-cycle of bacteriorhodopsin at room temperature. *FEBS Lett.* 292:73–75.

Oesterhelt, D., J. Tittor, and E. Bamberg. 1992. A unifying concept for ion translocation by retinal proteins. *J. Bioenerg. Biomembr.* 24:181–191.

Olson, K. D., P. Deval, and J. L. Spudich. 1992. Absorption and photochemistry of sensory rhodopsin-I: pH effects. *Photochem. Photobiol.* 56:1181–1187.

Olson, K. D., and J. L. Spudich. 1993. Removal of the transducer protein from sensory rhodopsin I exposes sites of proton release and uptake during the receptor photocycle. *Biophys. J.* 65:2578–2585.

Olson, K. D., X-N. Zhang, and J. L. Spudich. 1995. Residue replacements of buried aspartyl and related residues in sensory rhodopsin I: D201N produces inverted phototaxis signals. *Proc. Natl. Acad. Sci. USA.* 92: 3185–3189.

Otto, H., T. Marti, M. Holze, T. Mogi, M. Lindau, H. G. Khorana, and M. P. Heyn. 1989. Aspartic acid-96 is the internal proton donor in the reprotonation of the Schiff base of bacteriorhodopsin. *Proc. Natl. Acad. Sci. USA.* 86:9228–9232.

Otto, H., T. Marti, M. Holz, T. Mogi, L. J. Stern, F. Engel, H. G. Khorana, and M. P. Heyn. 1990. Substitution of amino acids Asp-85, Asp-212, and Arg-82 in bacteriorhodopsin affects the proton release phase of the pump and the pKa of the Schiff base. *Proc. Natl. Acad. Sci. USA.* 87:1018–1022.

Rao, M. N., A. A. Kembhavi, and A. Pant. 1996. Implication of tryptophan and histidine in the active site of endo-polygalacturonase from *Aspergillus ustus*: elucidation of the reaction mechanism. *Biochim. Biophys. Acta.* 1296:167–173.

Rath, P., K. D. Olson, J. L. Spudich, and K. J. Rothschild. 1994. The Schiff base counterion of bacteriorhodopsin is protonated in sensory rhodopsin I: spectroscopic and functional characterization of the mutated proteins D76N and D76A. *Biochemistry.* 33:5600–5606.

Rath, P., E. N. Spudich, D. D. Neal, J. L. Spudich, and K. J. Rothschild. 1996. Asp76 is the Schiff base counterion and proton acceptor in the proton translocating form of sensory rhodopsin I. *Biochemistry.* 35: 6690–6696.

Ren, X., C. Tu, P. J. Laipis, and D. N. Silverman. 1995. Proton transfer by histidine 67 in site-directed mutants of human carbonic anhydrase III. *Biochemistry.* 34:8492–8498.

Rothschild, K. J. 1992. FTIR difference spectroscopy of bacteriorhodopsin: toward a molecular model. *J. Bioenerg. Biomembr.* 24:147–167.

Sheikh, S. P., T. A. Zvyaga, O. Lichtarge, T. P. Sakmar, and H. R. Bourne. 1996. Rhodopsin activation blocked by metal-ion-binding sites linking transmembrane helices C and F. *Nature.* 383:347–350.

Shimoni, E., E. Nachliel, and M. Gutman. 1993. Gaugement of the inner space of the apomyoglobin's heme binding site by a single free diffusing proton. II. Interaction with a bulk proton. *Biophys. J.* 64:480–483.

Spudich, J. L. 1994. Protein-protein interaction converts a proton pump into a sensory receptor. *Cell.* 79:747–750.

Spudich, J. L., and R. A. Bogomolni. 1984. The mechanism of colour discrimination by a bacterial sensory rhodopsin. *Nature.* 312:509–513.

Spudich, E. N., and J. L. Spudich. 1993. The photochemical reactions of sensory rhodopsin I are altered by its transducer. *J. Biol. Chem.* 268: 16095–16097.

Spudich, E. N., S. A. Sundberg, D. Manor, and J. L. Spudich. 1986. Properties of a second sensory receptor protein in *Halobacterium halobium* phototaxis. *Proteins Struct. Funct. Genet.* 1:239–246.

Spudich, E. N., W. Zhang, M. Alam, and J. L. Spudich. 1997. Constitutive signaling by the phototaxis receptor sensory rhodopsin II from disruption of its protonated Schiff base-Asp-73 interhelical salt bridge. *Proc. Natl. Acad. Sci. USA.* 94:4960–4965.

Steinhoff, H. J., R. Mollaaghababa, C. Altenbach, K. Hideg, M. Krebs, H. G. Khorana, and W. L. Hubbell. 1994. Time-resolved detection of structure changes during the photocycle of spin-labeled bacteriorhodopsin. *Science.* 266:105–107.

Subramaniam, S., M. Gerstein, D. Oesterhelt, and R. Henderson. 1993. Electron diffraction analysis of structural changes in the photocycle of bacteriorhodopsin. *EMBO J.* 12:1–8.

Subramaniam, S., D. A. Greenhalgh, and H. G. Khorana. 1992. Aspartic acid 85 in bacteriorhodopsin functions both as proton acceptor and negative counterion to the Schiff base. *J. Biol. Chem.* 267:25730–25733.

Tittor, J., Ch. Söll, D. Oesterhelt, H.-J. Butt, and E. Bamberg. 1989. A defective proton pump, point-mutated bacteriorhodopsin Asp96→Asn is fully reactivated by azide. *EMBO J.* 8:3477–3482.

Vonck, J. 1996. A three-dimensional difference map of the N intermediate in the bacteriorhodopsin photocycle: part of the F helix tilts in the M to N transition. *Biochemistry.* 35:5870–5878.

Yan, B., and J. L. Spudich. 1991. Evidence that the repellent receptor form of sensory rhodopsin I is an attractant signaling state. *Photochem. Photobiol.* 54:1023–1026.

Yao, V. J., E. N. Spudich, and J. L. Spudich. 1994. Identification of distinct domains for signaling and receptor interaction of the sensory rhodopsin I transducer, HtrI. *J. Bacteriol.* 176:6931–6935.

Zhang, W., A. Brooun, M. M. Müller, and M. Alam. 1996. The primary structures of the archaeon *Halobacterium salinarium* blue light receptor sensory rhodopsin II and its transducer, a methyl-accepting protein. *Proc. Natl. Acad. Sci. USA.* 93:8230–8235.